Available online at www.sciencedirect.com
ScienceDirect
Earth and Planetary Science Letters 251 (2006) 334–345
EPSL
www.elsevier.com/locate/epsl

Terrestrial manganese-53 — A new monitor of Earth surface processes

Joerg M. Schaefer [a,*], Thomas Faestermann [b], Gregory F. Herzog [c], Klaus Knie [b], Gunther Korschinek [b], Jozef Masarik [d], Astrid Meier [b], Michail Poutivtsev [b], Georg Rugel [b], Christian Schlüchter [e], Feride Serifiddin [c,1], Gisela Winckler [a]

[a] *Lamont-Doherty Earth Observatory, Route 9W, Palisades, NY-10964, USA*
[b] *Technische Universität München, Fakultät für Physik E15, 85748 Garching, Germany*
[c] *Rutgers University, Department of Chemistry and Chemical Biology, 610 Taylor Road, Piscataway, NJ 08854-8087, USA*
[d] *Commenius University Bratislava, Department of Nuclear Sciences, Bratislava, Slovakia*
[e] *Universität Bern, Geologisches Institut, CH-3012 Bern, Switzerland*

Received 20 June 2006; received in revised form 1 September 2006; accepted 5 September 2006
Available online 12 October 2006
Editor: H. Elderfield

Abstract

We report the first systematic study of the terrestrial cosmogenic radionuclide manganese-53 ($T_{1/2}$=3.7 Ma) measured in thirteen samples from nine dolerite surfaces in the Dry Valleys, Antarctica. The terrestrial manganese-53 concentrations correlate well with cosmic-ray-produced helium-3 and neon-21 concentrations in the same samples, implying that the manganese-53 is produced continuously in situ and retained quantitatively over millions of years. The terrestrial manganese-53 production rate determination normalized to iron (the only important target element) and to high-latitude and sealevel yields a value of P_{53}=103±11 atoms yr^{-1} (g Fe)$^{-1}$. This is consistent with the theoretical value of 120±18 atoms yr^{-1} (g Fe)$^{-1}$ obtained from modeling calculations. Our results show that the manganese-53 concentrations in bulk terrestrial rocks can be used to monitor Earth surface processes on time-scales exceeding 10 My.

Keywords: terrestrial cosmogenic nuclides; Earth surface processes; radionuclides; accelerator mass spectrometry; Dry Valleys; Antarctica

1. Introduction

Terrestrial Cosmogenic Nuclides (TCN) have become indispensable tools in the earth sciences, particularly for studying the chronology of landforms [1–3]. Recent rapid progress in the TCN method has expanded the dating time-scale, improved analytical precision, extended the range of datable lithologies to include whole rocks, led to more precise production rates, and widened the spectrum of useful cosmogenic nuclide systems (e.g. [4,5]). Here we report a methodical investigation of terrestrial manganese-53 ($T_{1/2}$=3.7 Ma) – a nuclide that so far has seen almost exclusively extraterrestrial applications – in rocks from the Dry Valleys, Southern Victoria Land, Antarctica.

* Corresponding author. Tel.: +1 845 365 8703; fax: +1 845 365 8155.
E-mail address: schaefer@ldeo.columbia.edu (J.M. Schaefer).
[1] Current address: Space Science Laboratory, UC Berkeley, CA 94720-7450.

0012-821X/$ - see front matter © 2006 Elsevier B.V. All rights reserved.
doi:10.1016/j.epsl.2006.09.016

Cosmogenic ^{53}Mn was first measured in extraterrestrial materials by low-level counting techniques (see [6,7]). In 1965, a more sensitive method based on neutron activation was introduced by Millard [8]. It quickly supplanted low-level counting, ushering in a period that lasted through the mid-1990s (e.g., [9–12]). Although considerably easier than low-level counting, Millard's method requires sophisticated radiochemistry. Therefore only very few ^{53}Mn analyses of terrestrial samples have been reported (e.g. [13]). Progress in measuring ^{53}Mn by accelerator mass spectrometry (AMS) [14], increasing the sensitivity by two orders of magnitude, suggested to us that the time had arrived for the systematic study of terrestrial ^{53}Mn. Our initial goals were 1) to demonstrate the presence of cosmogenic ^{53}Mn in terrestrial rocks; 2) to see whether ^{53}Mn is conserved in rocks, a key requirement for dating; 3) to determine a ^{53}Mn production rate; and 4) to compare the experimentally measured production rate with a value derived from theoretical calculations.

We selected for this study a suite of dolerite rocks from the Dry Valleys, Antarctica. Earlier studies had shown that these rocks contain some of the highest cosmogenic ^{3}He and ^{21}Ne concentrations known for

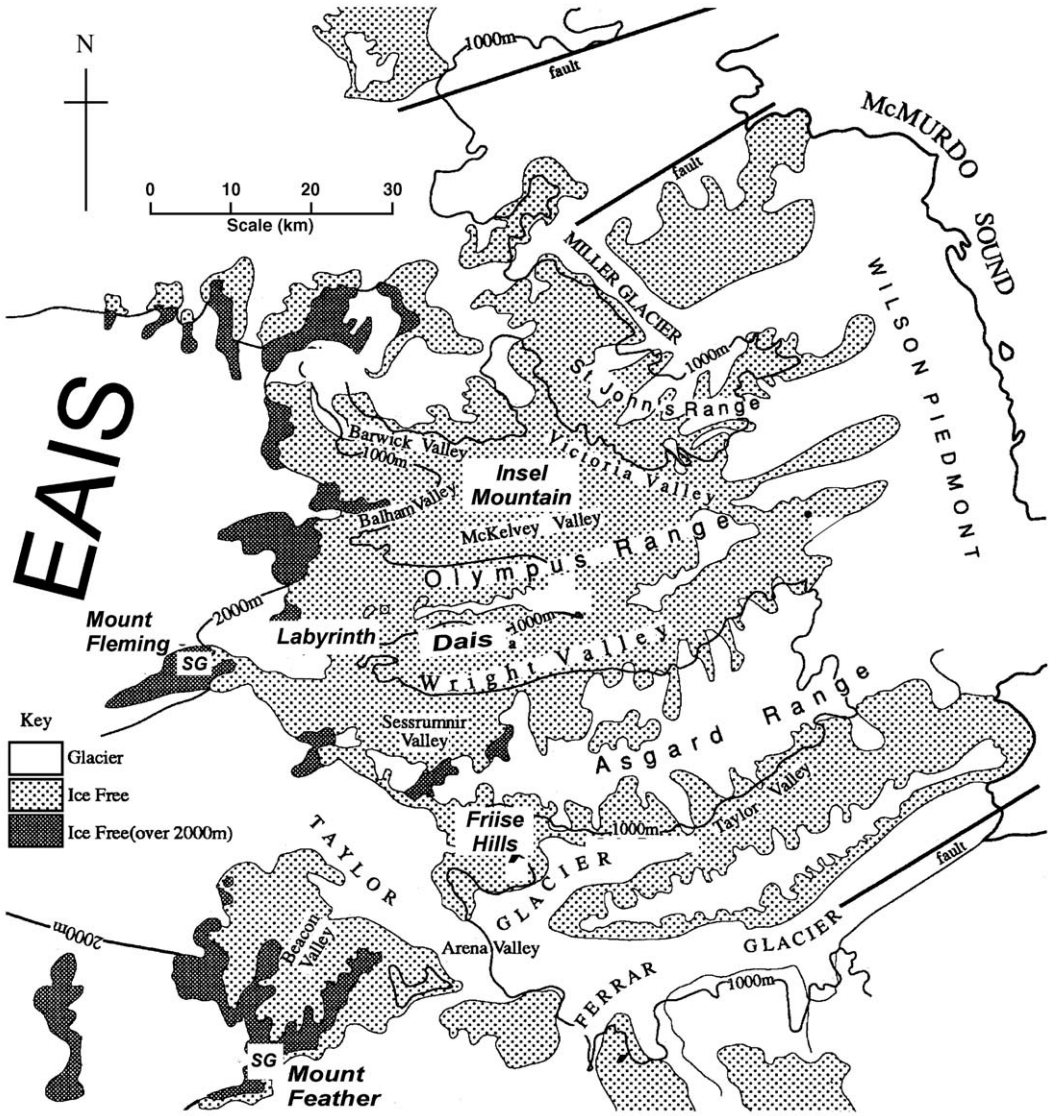

Fig. 1. Map of the Dry Valleys, Antarctica. The map is modified after [20] giving the sample sites. SG = Sirius Group sediment locations; EAIS = East Antarctic Ice Sheet. Samples 318 and NXP are from the SG at Mt. Fleming and Mt. Feather, respectively; Samples 446s, 446B and 464 from Insel Mt.; Sample 444 from the Labyrinth; Samples 435 and 439 from the Dais; and sample 403 from the Friise Hills.

any terrestrial samples [15]. These observations suggested that the ^{53}Mn concentrations of the rocks would also be large, and therefore relatively easy to measure. We cross-calibrate the terrestrial ^{53}Mn production rate by comparing the ^{53}Mn concentrations of each sample to the cosmogenic ^{3}He concentrations and the respective cosmogenic ^{3}He production rate, which is one of the best calibrated production rates for any TCN [1,16].

If TCNs are to be useful in dating, their host lithologies must not exchange with the surroundings either the TCN themselves or the elements from which they are made. To see whether ^{53}Mn and its principal parent, iron, met this requirement for our samples, we analysed both whole-rock samples and mineral separates.

Preliminary versions of this work have appeared in abstracts, e.g. [17,18].

2. Methods

2.1. Samples

Fig. 1 shows the field area. The samples are from erratic boulders that are elements of the Sirius Group tillites at Mt. Fleming (318) and Mt. Feather (NXP) and from bedrock samples from the Inner Dry Valleys including the Labyrinth (444), the Dais (435, 439), the Friise Hills (403), and the Insel Mountain (464, 446s and 446B; the last two samples were taken from the same geomorphological unit). For more details concerning sample collection see [15]; for detailed geomorphology of the Dry Valleys see e.g. [19,20].

The lithology of all rocks is Ferrar Dolerite, consisting primarily of pyroxene and plagioclase. Pyroxene separation is performed using standard magnetic and heavy liquid techniques followed by hand-picking (for details see [15]).

For all samples except 446B, cosmogenic helium and neon data were reported earlier [15]. To compare terrestrial ^{53}Mn and cosmogenic noble gas concentrations from aliquots of the same sample, we resampled all rocks and split the samples after crushing into fractions for manganese and helium measurement.

2.2. Noble gas analyses

We reanalysed pyroxene separates from the helium fractions of all samples (318, NXP, 446s, 446B, 464, 403, 435, 439, 444) for helium isotopes at the noble gas facility at the Lamont-Doherty Earth Observatory (LDEO) [21,22]. Samples are heated to ~1300–1400 °C for 15 min for total gas extraction. The released gases are exposed to a liquid nitrogen cooled charcoal trap to freeze out permanent gases such as water vapor, oxygen and CO_2. The gas is further purified by exposure to a SAES getter at room temperature to minimize the hydrogen background. The residual gas is collected on a cryogenically cooled trap held at ~13 K. Helium is released into the mass spectrometer by heating the trap to 45 K while heavier noble gases remain frozen to the cold trap. Helium concentration and isotopic composition measurements are performed on a MAP 215-50 noble gas mass spectrometer calibrated with a known volume of a Yellowstone helium standard (MM) with a ^{3}He/^{4}He ratio of $16.45R_a$, where $R_a=(^{3}He/^{4}He)_{air}=1.384\cdot10^{-6}$. Typical hot blanks yield ^{4}He concentrations of less than 10^{-10} cm^3 STP with approximately atmospheric helium isotopic signature, corresponding to ^{3}He blank corrections of <1%.

2.3. ^{53}Mn analyses

2.3.1. Chemistry

The chemical procedure used to separate manganese from terrestrial rocks is similar to those used for meteorites [23,24]. We analysed ^{53}Mn in five pyroxene separates, namely NXP-93-52, 446B-030404, 403-030404, 403-020904, and 444-030404, and in eight whole rock samples, namely 318-1, 318-2, NXP-022004, 446s-2, 464-011105, 435-102504, 435-022005, and 439-011105 (the latter part of the sample name indicates subsamples). A split of the whole rock and pyroxene samples for ^{53}Mn measurement is analysed for elemental composition. The samples (we used grain sizes between 200 and 500 μm, but all grain sizes including rock powder can be used) are weighed into teflon vessels. To achieve the desirable mass of manganese for accelerator mass spectrometry analysis (1 mg Mn minimum, 4 mg Mn desirable), we added stable Mn (Fisher Scientific ICP manganese; 1 mg/ml) as a carrier to samples with less than 1.5 mg natural manganese content (resulting in Mn masses between 1.7 and 6.1 mg). The sediment sample is dissolved in a closed Teflon vessel using a solution of hydrofluoric acid (HF), perchloric acid ($HClO_4$), and nitric acid (HNO_3) at 115 °C during 12 to 24 h. The digestion could also be done at lower temperature. Following dissolution, the sample is fumed with a mixture of 7 M hydrochloric acid (HCl) and concentrated $HClO_4$ to remove fluorides and chromium, the latter being a problematic interference in AMS analysis on atomic mass 53. Fuming is repeated twice more before the sample is loaded onto a standard anion column in 10.2 M HCl after including a trace of hydrogen peroxide (H_2O_2) [24]. The anion column chromatography is

repeated three times to remove traces of chromium. Manganese is precipitated with $KClO_3$ as MnO_2, dried, mixed with silver powder, and pressed into high purity silver target holders. From start to finish, the preparation of a MnO_2 AMS target from a dissolved rock sample typically takes 3 to 4 days.

2.3.2. Accelerator mass spectrometry

We measured ^{53}Mn concentrations at the Munich MP Tandem with the terminal voltage set to ~13 MV [25] (Fig. 2). A sputter ion source produces beams of MnO^- (typically a few 100 nA) that are mass selected, and injected into the tandem for further acceleration. At the terminal of the tandem, the $^{53}MnO^-$ ions pass through a thin carbon foil (~4 μg/cm^2) where a large fraction of the electrons is stripped off. This process leads to dissociation of all molecular ions. The resulting multiply charged positive ions are further accelerated by the same voltage as they exit the accelerator. Downstream, a 90° analysing magnet selects $^{53}Mn^{11+}$ ions with an energy of 156 MeV ($m/\Delta m \sim 10^4$), allowing an efficient suppression of fragments from molecular background. However, all these steps do not achieve separation of ^{53}Mn from its stable isobar ^{53}Cr. For this purpose we utilize a detector system consisting of a gas-filled magnet and a multi-anode ionisation chamber. Due to collisions with the gas particles in the magnet the average charge state of the ions depends on their nuclear charge. Consequently, the trajectories of ^{53}Cr and ^{53}Mn ions have different radii and exit the gas-filled magnet at different positions. Further isobaric separation is achieved in an ionisation chamber by measuring the ions' differential energy loss, which depends again on their nuclear charge. Interfering ^{53}Cr ions are suppressed by a factor of 10^3 in the gas-filled magnet and by a further factor of 10^6 in the ionisation chamber, where ^{53}Mn events are accepted with an efficiency of about 30% [25].

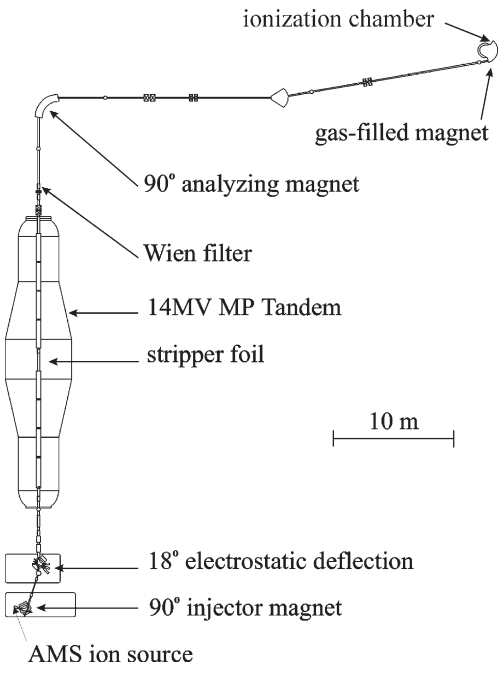

Fig. 2. Schematic set up of the MP Tandem AMS facility at the TU Munich.

^{53}Mn concentrations are measured relative to our laboratory standard "Grant GLS" which was prepared from the iron meteorite Grant. Its $^{53}Mn/^{55}Mn$ ratio, $(2.96 \pm 0.06) \cdot 10^{-10}$, has been determined by comparison with a primary standard produced in a nuclear reaction: Short-lived ^{53}Fe ($T_{1/2} = 8.51$ min) was produced via $^{54}Fe(^3He,\alpha)^{53}Fe$ at the Munich tandem accelerator. It is energetically not possible to produce ^{53}Mn directly since the ^3He particle energy was only 19 MeV. Therefore, all ^{53}Mn is due to radioactive decay of ^{53}Fe. The ^{53}Fe activity was measured by means of gamma ray spectroscopy (the efficiency of the gamma spectroscopy has been determined with an ^{152}Eu standard), yielding the number of initially produced ^{53}Fe nuclei after correction for radioactive decay. This number equals the number of ^{53}Mn nuclei in the primary standard after complete decay of the short-lived ^{53}Fe to ^{53}Mn.

For background determination, and, in turn, evaluation of the Cr suppression factors, we measured ^{53}Mn-free blanks made of commercial manganese with a Cr content comparable to our samples. Those yielded $^{53}Mn/^{55}Mn$ ratios of a few times 10^{-14}, which is between 10 and 280 times lower than our measured sample ratios (see Table 2). Typically, samples have been measured for 1–2 h each.

2.4. Calculations to model the rate of ^{53}Mn production on the earth's surface

For comparison with the measurements, we simulate ^{53}Mn production in terrestrial rocks with a computer model based on two published codes, GEANT [26] and MCNP [27]. As this model is described in detail elsewhere [28], we recount only its main features. For the primary particle flux, we consider protons with energies between 10 MeV and 100 GeV. The primary flux is set equal to the long-term average value of 4.56 p cm^{-2} s^{-1} determined from cosmogenic nuclide data in lunar samples [29].

Table 1
Cosmogenic noble gas data

Sample	Subsample	$^{21}Ne_{cos}$ (10^6 at g^{-1})§	^{21}Ne-age (My)§	^{3}He (10^9 at g^{-1})§	^{3}He-age (My)§	^{3}He (10^9 at g^{-1})£	^{3}He-age (My)£
318	1	–	–	–	–	6.09±0.15	6.75±0.17
318	2	1623±52	8.16±0.16	6.90±0.27	7.64±0.30	–	–
NXP	93-52						
		1557±55	4.27±0.15	5.21±0.18	4.36±0.15	5.21±0.25&	4.36±0.23
NXP	022004						
446s	2	711±25	5.28±0.19	2.79±0.11	4.85±0.19	3.08±0.08	5.36±0.13
446B	030404	–	–	–	–	1.30±0.02	2.50±0.05
464	011105	522±18	4.50±0.16	2.36±0.09	4.16±0.16	2.78±0.07	4.89±0.12
435	102504						
		391±12	3.16±0.10	1.85±0.07	3.05±0.12	2.28±0.06	3.77±0.09
435	022005						
403	030404						
		340±11	2.45±0.08	1.49±0.04	2.19±0.09	1.34±0.06	1.97±0.08
403	020904						
439	011105	261±9	3.52±0.12	1.00±0.04	3.01±0.11	0.92±0.02	2.79±0.05
444	030404	124±6	1.27±0.06	0.53±0.02	1.25±0.06	0.52±0.02	1.23±0.05

Noble gas data are given within 1σ uncertainties including counting statistics and sensitivity variations of the mass-spectrometer.
§: Noble gas data from pyroxene by [15], typical sample size about 200 mg. The updated ^{21}Ne production rates are based on the element concentrations given in [15] and on the updated elemental production rates given by [45]. The ^{3}He production rates are based on a sealevel/high latitude value of 115 at g^{-1} yr^{-1}. The slhl production rate values were scaled to the sample locations using the procedure given in [30] including neutron and muon production, taking into account the Antarctic sealevel air pressure (989 hPa instead of 1013 hPa), resulting in about 25% younger ages than previously published.
£: Pyroxene samples reanalysed for helium isotopes at the noble gas laboratory at the Lamont-Doherty Earth Observatory using pyroxene separates from the same samples measured for ^{53}Mn. Typical sample size is about 20 mg. Production rate systematics: see section § above.
&: reported ^{3}He concentration is the mean within 1σ standard deviation of nine ^{3}He analysis of sample NXP.

We calculate the propagation of primary particles and their production of secondary protons and neutrons. All particles are followed through the atmosphere and into the lithosphere. For this purpose, the atmosphere is modeled as a spherical shell with an inner radius of 6378 km and a thickness of 100 km.

Table 2
Terrestrial ^{53}Mn results from pyroxene and whole rock samples together with iron and manganese concentration data

Sample	Subsample	Sample type	Altitude (m)	Sample mass (g)	Mn (wt.%)	^{55}Mn carrier (mg)	Fe (wt.%)	^{53}Mn/^{55}Mn (10^{-12})	^{53}Mn (10^9 atoms (g Fe)$^{-1}$)
318	1	wr	2150	1.026	0.15	2.2602	7.83	6.56±0.98	3.37±0.50
318	2	wr	2150	3.012	0.14	–	7.27	15.3±2.18	3.21±0.46
NXP	93-52	Px.	2555	1.052	0.16	–	7.04	12.7±0.9	3.16±0.22
NXP	022004	wr	2555	1.500	0.14	–	6.54	13.9±2.0	3.36±0.49
446s	2	wr	1530	1.033	0.15	2.4235	7.20	2.8±0.6	1.62±0.35
446B	030404	Px	1530	1.996	0.17	–	5.54	6.2±1.4	2.09±0.46
464	011105	wr	1515	0.223	0.17	2.027	7.63	2.0±0.4	3.15±0.55
								+0.16	+0.61
435	102504	wr	1595	0.102	0.19	2.990	9.21	0.41	1.52
								−0.14	−0.52
435	022205	wr	1595	0.162	0.19	3.031	9.21	0.51±0.14	1.25±0.34
403	030404	Px	1750	2.001	0.31	–	10.11	5.7±0.9	1.91±0.29
403	020904	Px.	1750	1.001	0.31	–	11.84	5.1±1.1	1.47±0.31
439	011105	wr	869	0.201	0.19	2.020	8.29	0.47±0.2	0.74±0.36
								+0.5	+0.12
444	030404	Px	1145	2.000	0.30	–	13.35	1.4	0.34
								−0.4	−0.09

^{53}Mn/^{55}Mn ratios reflect AMS measured values. Errors represent 1σ statistical uncertainty.
Manganese and iron concentrations were measured at Rutgers University by Atomic Absorption Spectrometry and for some samples additionally by ICP-MS.
wr: 'whole rock'; Px: 'pyroxene'.
If the detected counts are below 20, uncertainties are calculated following an approach including Poisson statistics developed for experiments with small signals and known background [46].

Atmospheric composition (by weight) is assumed to be: 75.5% N, 23.2% O, and 1.3% Ar. The total thickness of the atmosphere is taken to be 1033 g cm^{-2}. For the Earth's surface, we assume the following average elemental composition (by weight): 0.2% H, 47.3% O, 2.5% Na, 4.0% Mg, 6.0% Al, 29.0% Si, 5.0% Ca and 6.0% Fe. Reasonable changes to this surface composition, e.g., addition of K, have little effect on the calculated fluxes, although hydrogen is an exception in this regard. The surface density of the Earth is set at 2.0 g cm^{-3}. To investigate the depth dependence of particle fluxes, the near-subsurface region is divided into spherical shells, each with a thickness of 5 g cm^{-2}. We calculate the fluxes of protons and neutrons within each cell. The statistical errors of the calculations are approximately 5–8%. Uncertainties of the calculated fluxes are estimated to be in the range of 5–10% for depths less than 400 g cm^{-2} and to increase with depth. Having calculated the particle fluxes, the production rates of ^{53}Mn are calculated by integrating over energy the product of these fluxes and cross-sections for the nuclear reactions that produce the ^{53}Mn. As suggested above, nuclear reactions with ^{56}Fe are by far the most important source of ^{53}Mn production.

3. Results

New cosmogenic ^{3}He results are shown in Table 1 together with cosmogenic ^{3}He and ^{21}Ne data published earlier [15]. The ^{53}Mn data are given in Table 2. The data sets are compared in Fig. 3, and the terrestrial ^{53}Mn

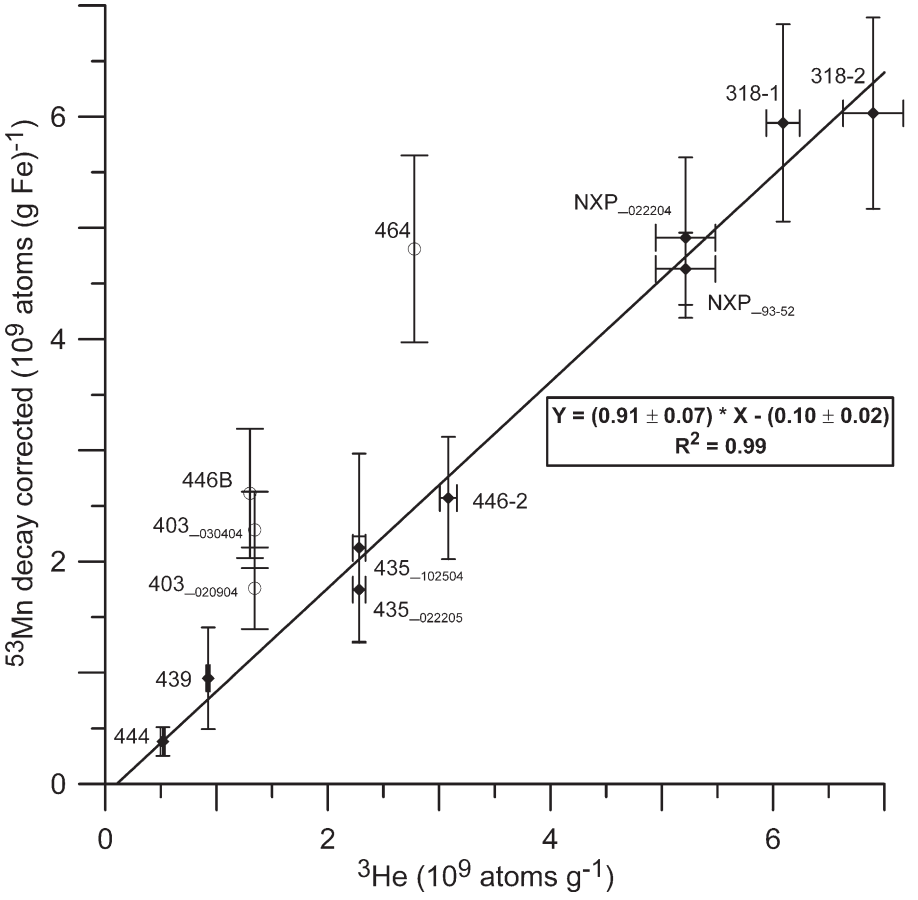

Fig. 3. Cosmogenic ^{53}Mn–^{3}He scatter plot. 'Decay correction' for ^{53}Mn concentrations are based on $(^{53}Mn)_{decay-corr}=(^{53}Mn)_{measured}\cdot(\lambda T_{21}/(1-e^{-\lambda T}))$, where $\lambda=0.187\cdot10^{-6}$ a^{-1} and $T=^{3}$He-age (yr); For all samples but 318-2, ^{53}Mn and ^{3}He concentrations were measured on aliquots from the same samples, i.e. we used the new ^{3}He data presented here to cross-calibrate the ^{53}Mn production rate in Fig. 3 (^{3}He data marked with "§" in Table 1). The ^{53}Mn concentration of sample 318-2 is measured from an aliquot of the sample that was measured earlier for cosmogenic ^{3}He and ^{21}Ne [15], i.e. for this samples we used the earlier ^{3}He concentration in Fig. 1 (^{3}He data marked with "£" in Table 1). The filled diamonds indicate the data used for the ^{53}Mn–^{3}He production rate cross-calibration and fitted by the regression ($R^2=0.99$). The slope of 0.91±0.07 reflects the production rate ratio of cosmogenic ^{53}Mn/^{3}He. Samples 446B, 403, and 464 (open circles) are not used for cross-calibration (see Section 3.1).

production rate cross-calibration is shown in Fig. 3 and Table 3.

3.1. Cosmogenic noble gases

Table 1 shows cosmogenic noble gas exposure age calculations assuming no erosion and hence yielding minimum exposure ages. Production rates are based on the scaling procedure given by Stone [30], taking into account the Antarctic sealevel air pressure (989 hPa instead of 1013 hPa), resulting in about 25% younger minimum ages than previously published [15]. The new minimum ^{3}He-ages range from 1.2±0.1 My (444) to 6.8±0.2 My (318) (Table 1; last column), the ^{3}He exposure ages recalculated from the earlier data range from 1.3±0.1 My (444) to 7.6±0.3 My (318) (Table 1; column six). The new ^{3}He concentrations agree with the earlier helium data for samples NXP, 446s, 464, 435 and 444. The new ^{3}He concentrations and ages measured from samples 403, 446B, and 439 are about 20% younger than the earlier ^{21}Ne-age and about 10% younger than the ^{3}He-ages given in [15]. As mentioned above, sample 446B is taken from the same geomorphological unit and only a few meters away from sample 446s. The two exposure ages should agree. In fact, the new ^{3}He-age of 446B of 2.5 My is only half of the ^{21}Ne (5.3±0.2 My) and ^{3}He-age (4.9±0.2 My) of the geomorphological sister sample 446s.

Pyroxene from Ferrar Dolerite has been proven to be retentive for cosmogenic ^{3}He on long time-scales [15,31], and therefore cannot be blamed for the lower ^{3}He-ages compared to the ^{21}Ne-ages. However, plagioclase loses >90% of all cosmogenic ^{3}He by diffusion on time-scales discussed here, whereas more than half of the cosmogenic ^{21}Ne is retained [32]. Thus, the lower ^{3}He-ages are most easily explained by ^{3}He loss from plagioclase present in the pyroxene separates. Plagioclase contamination of pyroxene separates is a known problem for Ferrar Dolerite samples (e.g. [33,34]). X-ray diffraction analysis for samples 318, NXP, 446s, 464, 435,

Table 3
Measured and modelled ^{53}Mn production rates

Sample	Subsample	Sample type	Local ^{53}Mn prod. rate (atoms yr^{-1} (g Fe)$^{-1}$)	^{53}Mn prod. rate, sealevel (atoms yr^{-1} (g Fe)$^{-1}$)
318	1	wr	880±133	112±17
318	2	wr	836±121	107±15
NXP	93-52	Px	1060±93	102±9
NXP	022004	wr	1120±175	108±17
446s	2	wr	479±103	96±21
435	102504	wr	563±225	107^{+43}_{-37}
435	022205	wr	463±127	88±24
439	011105	wr	340±164	118^{+57}_{-48}
444	030404	Px	311±106	85^{+29}_{-23}
Unweighted mean				**103±11**
Weighted mean				**103±6**
Theoretical value				**120±18**
446B (^{3}He-age)	030404	Px	1130±262	<226±52
446B (^{21}Ne-age of 446s)		Px	622±140	123±28
403	030404	Px	1160±181	<196±31
403	020904	Px	893±190	<151±32

Measured production rates are calculated using the measured ^{53}Mn concentrations (Table 2) decay-corrected with the ^{3}He exposure age derived from the same sample given in Table 1. We used $\lambda = 0.187 \cdot 10^{-6}$ a^{-1} (corresponding to $t_{1/2}$=3.7 Ma).
Uncertainties reflect the 1σ error of the ^{53}Mn and ^{3}He concentrations given in Table 2. We give the local production rate values at the sample location together with the sealevel production rates using the scaling procedure given in [30] based on Antarctic atmosphere pressure (sealevel air pressure of 989 hPa). We include the upper nine samples to determine a ^{53}Mn production rates that are given as mean within 1σ standard deviation and as weighted mean, respectively (see also Fig. 3). Samples 403 and 446B are used to calculate an upper limit for the ^{53}Mn production rate.

439, and 444 indicated that the separates were relatively clean consisting of more than 90% pyroxene. However, the pyroxene separates of samples 446B and 403 were found to contain significant amounts of plagioclase [35]. For the ^{53}Mn–^{3}He cross-calibration presented below, we therefore exclude samples 403 and 446B and use the data only to determine upper limits for the ^{53}Mn production rate (Table 3).

3.2. AMS measurements of ^{53}Mn

The results of the AMS ^{53}Mn concentration measurements given in Table 2 (together with natural iron and manganese concentrations and amounts of ^{55}Mn added as carrier) range from $3.4\cdot10^{8}$ (444) to $3.4\cdot10^{9}$ atoms (g Fe)$^{-1}$ (318-1 and NXP-022004). The ^{53}Mn/^{55}Mn ratios range from $0.4\cdot10^{-12}$ to $15\cdot10^{-12}$, well above the background of about $0.05\cdot10^{-12}$. The good agreement between the ^{53}Mn concentrations measured in the pyroxene NXP-93-52 and the whole rock sample NXP-022004 implies that ^{53}Mn can be reliably measured from whole rock. The duplicate samples (318-1 and 318-2; 435-102504 and 435-022005; 403-020904 and 403-030404) indicate satisfactory reproducibility of the terrestrial ^{53}Mn measurements.

3.3. Evidence for in-situ production of ^{53}Mn

Under the assumption that the effects of erosion (see Section 3.4) and uplift [31] are small for the samples discussed here, the ^{53}Mn concentration normalized to iron concentration, [^{53}Mn], grows with exposure age, t, according to the relation

$$[^{53}\mathrm{Mn}] = P(^{53}\mathrm{Mn})/\lambda(1-e^{-\lambda t}) \quad (1)$$

while the ^{3}He concentration increases linearly with time

$$[^{3}\mathrm{He}] = P(^{3}\mathrm{He})t \quad (2)$$

Combining the two equations and rearrangement leads to

$$[^{53}Mn]\frac{\lambda t}{1-e^{-\lambda t}} = \frac{P(^{53}Mn)}{P(^{3}He)}[^{3}He] \quad (3)$$

where P is the production rate and λ is the decay constant for ^{53}Mn. For Eq. (3) to hold, the following conditions must be met: 1) cosmic-ray flux is constant over time, which requires minimal uplift; 2) irradiation geometry is fixed, which implies minimal erosion and no periods of burial; 3) manganese and iron do not exchange with the surroundings.

Since neither neutron energy spectrum nor cross-sections change appreciably over the relevant altitudes (850 m to 2500 m), we can assume that the ratio $\frac{P(^{53}\mathrm{Mn})}{P(^{3}\mathrm{He})}$ is constant within our sample set. This makes it straightforward to examine whether the ^{53}Mn concentrations in our samples vary as expected for in situ production, i.e. are consistent with Eq. (3).

Fig. 3 shows that this is indeed the case for the samples 318-1, 318-2, NXP-93-52, NXP-022004, 446s-2, 435-102504, 435-022205, 439-011105, and 444-030404. The colinearity of the data in ^{53}Mn/^{3}He-space suggests that ^{53}Mn is indeed in situ cosmic-ray-produced. For samples NXP-93-52 and 444 the ^{53}Mn analysis is done from a pyroxene separate, for all others whole rock is used, indicating that ^{53}Mn is produced and retained in whole rock and pyroxene over millions of years in the Antarctic.

Fig. 3 also shows outliers. The data for samples 403-030404, 403-020904, and 446B-030404 plot above the line, as noted above, consistent with ^{3}He loss from contaminant plagioclase. Sample 464-011105 also plots above the line, but ^{3}He and ^{21}Ne exposure ages agree for this sample (Table 1) and the X-ray diffraction analysis indicates a high purity of 97% pyroxene, so ^{3}He loss from plagioclase is not the reason. A possible explanation would be contamination by meteoritic, ^{53}Mn-rich, material during sample processing in the laboratory. Since we cannot rule this out, we do not further discuss this sample.

3.4. Experimental production rate of ^{53}Mn

A linear regression (R^2=0.99) through the 'calibration data points' 318-1, 318-2, NXP-93-52, NXP-022004, 446-2, 435-102504, 435-022205, 439-011105, and 444-030404, passes close to the origin (y-axis intercept=−0.10±0.02) and has a slope of 0.91±0.07, which equals the production rate ratio $\frac{P(^{53}\mathrm{Mn})}{P(^{3}\mathrm{He})}$ (Fig. 3).

Table 3 shows the experimentally derived ^{53}Mn production rate for each sample along with the corresponding theoretical result. The calculated ^{53}Mn production rates at sea level and high latitude for the calibration data range from 85±29 to 118±57 atoms yr^{-1} (g Fe)$^{-1}$, with an unweighted mean of 103±11 atoms yr^{-1} (g Fe)$^{-1}$. The samples with the depleted noble gas concentrations (but most likely non-depleted ^{53}Mn concentrations) 403-030404, 403-020904, and 446B yield upper bounds for the ^{53}Mn production rate of 196±31 atoms yr^{-1} (g Fe)$^{-1}$, 151±32 atoms yr^{-1} (g Fe)$^{-1}$ and 226±52 atoms yr^{-1} (g Fe)$^{-1}$, respectively (Table 3). If we calculate the ^{53}Mn

production rate for sample 446B using the cosmogenic noble gas age of its sister sample 446s (5.4 My instead of 2.5 My) the resulting value of $P(^{53}\mathrm{Mn}) = 123 \pm 28$ atoms yr^{-1} (g Fe)$^{-1}$ is in good agreement with the mean value given above.

3.4.1. The influence of erosion

The high minimum exposure ages of up to 7 My of our samples correspond to very low maximum erosion rates (assuming infinite exposure) of less than 10 cm/My. These samples are sensitive to the process of erosion (see Fig. 3 in [15]), so we evaluate the influence of erosion on the experimentally derived ^{53}Mn production rate. Assuming 2 cm/My of steady erosion for sample NXP-93-52 would increase the cross-calibrated ^{53}Mn production rate by 3%. Assuming 5 cm/My for this sample, a value close to the maximum erosion rate, yields a 9% higher ^{53}Mn production rate. For sample 444-030404, steady erosion at the rate of 10 cm/My would increase the ^{53}Mn production rate by not more than 2%. We conclude that our experimental determination of the terrestrial ^{53}Mn production rate is relatively robust against the process of steady erosion.

3.5. Theoretical calculation of the ^{53}Mn production rate

The modeled ^{53}Mn production rate for sea level and high-latitudes is 120 atoms yr^{-1} (g Fe)$^{-1}$, with an uncertainty of ~15%. This value is about 30% lower than that reported in an earlier modeling study [36]. Our calculations show that more than 99% of the terrestrial ^{53}Mn is produced from iron, in large measure because the concentrations of elements with $Z > 26$ were taken to be less than 1 wt.%, a situation typical for terrestrial rocks. The remaining 1% is produced by spallation reactions on manganese and copper. Neutron spallation at energies around 110 MeV dominates (est. > 95%). A small fraction (est. 3–5%) is also produced by muons. The size of the calculated production rate from iron shows that we can safely ignore primordial sources (a potential problem for ^{3}He), atmospheric sources (a potential problem for ^{10}Be, ^{21}Ne, and ^{38}Ar), and contributions from fission of U and Th (a potential problem for ^{21}Ne).

4. Discussion

4.1. Strengths of ^{53}Mn vis à vis other terrestrial cosmogenic nuclides

If manganese and iron were to behave conservatively in all minerals, then ^{53}Mn would be useful for rock chronometry wherever iron concentrations and production rates integrated over time were appreciable. Our data indicate that iron and manganese were conserved in the set of samples that we used to produce the first empirical calibration of the terrestrial ^{53}Mn production rate. Nishiizumi et al. [37] reported that Fe and Mn behaved conservatively in mineral fractions of Antarctic meteorites that had undergone different degrees of weathering. We conclude that in the Antarctic, manganese and iron seem to be conserved in surface rocks over time-scales relevant for cosmogenic dating studies. How well these observations generalize to other environments remains to be seen. Geochemists have known for a long time that manganese mobilizes easily under conditions of low pH and low oxygen availability [38], which would allow for fractionation. The size of the fractionation effect may be either small or localized, however. Jeon and Lee [39] studied the evolution of a soil column from granitic bedrock. They found that iron and manganese 'remained immobile during chemical weathering,' although they then point out that manganese concentrates at the bottom of the soil column. We anticipate that ^{53}Mn will be most reliable where weathering is slow, pH high, and oxygen readily available or water excluded.

Under such conditions ^{53}Mn dating should have particular advantages, some of which are complementary to those of terrestrial cosmogenic nuclides that are already widely used (^{10}Be, ^{26}Al, ^{36}Cl, ^{14}C, ^{3}He, and ^{21}Ne). First, for the measurement of in situ ^{10}Be, ^{26}Al, and ^{14}C, the preparation and analysis of quartz mineral separates is strongly preferred. For ^{53}Mn, as for ^{36}Cl, most whole rocks are suitable. Second and as noted above, the production of ^{53}Mn in whole rock samples is dominated by spallation from the single target element, iron, and is therefore much simpler than the complex whole rock production pathways for ^{36}Cl [40–42]. The relative simplicity of the production rate systematics should help in interpreting measurements and in comparing results for different samples. Third, the ^{53}Mn method can be applied to exposure time-scales exceeding 10 My. Fourth, since there is no significant non-cosmogenic source of ^{53}Mn, no sample decontamination or data deconvolution is necessary. Fifth, the chemical procedure to extract manganese from whole rock is relatively simple, making the sample preparation quick and relatively inexpensive. We expect a combination of additional production rate cross-calibration studies using different TCNs, laboratory cross-section experiments, and theoretical calculations will soon result in more accurate production rate estimates for ^{53}Mn.

The ^{53}Mn method introduced here is expected to be relevant to various earth scientific applications. In this

study, ^{53}Mn has been used to date surface exposures from 1–7 My. This timeframe can be straightforwardly extended up to 15 My. The combination of the long-lived radionuclide ^{53}Mn with cosmogenic noble gases should be useful for deciphering long-term geomorphic processes in slowly denudating landscapes. Erosion rates on time-scales of 10 My can now be quantified. Burial histories of bedrock subjected to lengthy periods of exposure and burial can now be reconstructed. Obvious targets for this approach include the bedrock underlying the ice-shields of Greenland and Antarctica, where the ^{53}Mn-technique can contribute to understanding when and for how long the polar continents were ice free in the recent geological past.

The new AMS ^{53}Mn technique is also expected to be relevant to the meteorite community [23,43]. The higher sensitivity would be of interest for very small samples and eventually might allow ^{53}Mn analysis of cosmic dust and other materials returned from space missions.

4.2. Current limitations of the ^{53}Mn method

Although several factors constrain the ^{53}Mn method as presented here, the most significant one is the counting rate of ^{53}Mn, typically 1 cpm for a sample with a ^{53}Mn/^{55}Mn ratio of $1 \cdot 10^{-12}$, 500 cpm for a standard with a ^{53}Mn/^{55}Mn ratio of $3 \cdot 10^{-10}$, and 0.03 cpm for a blank with a comparable Cr content than our samples. For practical counting times – on the order of 1 to 2 h – these rates translate into a statistical uncertainty of ~15% for Antarctic surfaces at 1000 m altitude containing 7 wt.% Fe and 0.2 wt.% Mn, that have been continuously exposed for 1 My. In addition, there is a systematical uncertainty between 5 and 10%. The uncertainty decreases as exposure duration, altitude, and iron content increase or Mn content decreases. We present calculations of expected ^{53}Mn/^{55}Mn ratios in a few specific types of sample in Section 5.

In principle, an overall reduction in uncertainty could be attained by counting for longer times, but only at appreciable cost in accelerator time. With accelerator time scarce and costly, this option is unlikely to be exercised except for samples of unusual scientific importance. Omission of ^{55}Mn carrier would facilitate AMS by raising the ^{53}Mn/^{55}Mn ratio. However, it would also require processing a larger sample mass to achieve the minimum of the few mg of Mn needed for AMS analysis. This would add to the difficulty of the chemical separation of manganese from rock samples on the order of 10 g or more.

On the accelerator side, improvements in counting rates may be achievable by improving transmission, increasing the ion source current and by decreasing the background due to Cr. Currently about 70–80% of the 'good' ^{53}Mn counts are rejected to suppress the ^{53}Cr background. Lower chromium levels would directly improve statistics and lower uncertainties. Our group is currently working towards these ends.

4.3. Geomorphologic implications

The agreement between cosmogenic ^{3}He and ^{53}Mn data presented here has implications for the ongoing discussion about the long-term landscape stability of the Dry Valleys. The very old cosmogenic noble gas exposure ages of the Dry Valleys samples were used to support the argument towards a stable East Antarctic Ice Sheet throughout the Pliocene period [15]. This is challenged by the controversial view that the EAIS melted almost entirely about 2.5–3 My ago (e.g. [44]) in response to the mid-Pliocene warm period, an apparent contradiction to the high exposure ages. However, the high cosmogenic noble gas concentrations of these surfaces could have been accumulated during several periods of exposure, at their current position or elsewhere, that were interrupted by periods of burial, e.g. by the EAIS. In this case the old noble gas exposure ages would not contradict a rather instable and fluctuating EAIS during Pliocene time. With the addition of a radionuclide measurement, however, it becomes possible, in principle, to identify samples that were exposed/buried intermittently. Such samples should show lower ratios of ^{53}Mn to stable cosmogenic nuclides than continuously exposed samples, since the radionuclide decays during the coverage while the concentrations of stable cosmogenic nuclides remain constant.

The observed agreement of the cosmogenic ^{53}Mn and noble gas concentrations argues against a significant burial time of these surfaces of 1 My or more. The data supports a simple and continuous exposure history of the Sirius Group and Inner Dry Valley bedrock surfaces. Exposure ages assign indeed minimum ages to the surface formation, ranging from more than 1 My for the Labyrinth, over approximately 5.4 My for the Insel Mountains to at least 6.8 My and 4.4 My for the Sirius Formations on Mt. Fleming and Mt. Feather, respectively. Therefore, this calibration study of terrestrial ^{53}Mn, in turn, supports the earlier geomorphic conclusions towards long-term stability of the EAIS given in [15], that were based on the cosmogenic noble gas data.

5. Conclusions

By using accelerator mass spectrometry, we have determined the concentrations of ^{53}Mn in Antarctic surface rocks with cosmogenic noble gas exposure ages ranging from 1.2 My to 7.6 My. In general, the ^{53}Mn concentrations increase with noble gas exposure age in the way one would expect if the sampled surfaces had simple histories of exposure to cosmic rays, a single stage of cosmic-ray irradiation in a fixed geometry. Regression analysis of these data with adjustments for altitude leads to an average ^{53}Mn production rate at sea level and high latitude of 103 ± 11 atoms yr^{-1} (g Fe)$^{-1}$. The experimental determination of the terrestrial ^{53}Mn production rate agrees well with a theoretically derived value of 120 ± 18 atoms yr^{-1} (g Fe)$^{-1}$.

Due to the abundance of Fe in rocks, ^{53}Mn, in principle, should be measurable in whole rock samples from most lithologies. The dating time-scale for ^{53}Mn is lithology dependent. Rocks with higher Fe/Mn ratios such as basalt and gabbro are preferable because they have higher intrinsic ^{53}Mn/^{55}Mn ratios, which are easier to measure by accelerator mass spectrometry. For example, a 5 g sample from basaltic rock (Fe $\approx$ 9 wt.%, Mn $\approx$ 0.14 wt.%) exposed for 0.5 My in Antarctica at 1500 m altitude would yield about 7 mg of manganese and a ratio of ^{53}Mn/^{55}Mn $= 2 \cdot 10^{-13}$, i.e. would be datable. Quartz-bearing rocks are attractive because they permit multi-nuclide dating with ^{53}Mn in concert with ^{10}Be, ^{26}Al, and ^{21}Ne. With the same parameters as above, however, a granitic sample (Fe $\approx$ 1.9 wt.%; Mn $\approx$ 0.04 wt.%) would yield only 2 mg of manganese and a ratio of ^{53}Mn/^{55}Mn $= 1.5 \cdot 10^{-13}$. Thus for granitic rocks a mass of 10 g would be required to reach the desired sample size of 4 mg manganese without adding manganese carrier.

If we can show that mobilization of iron and manganese in rocks over relevant time-scales of millions of years or less is small even in humid environments, then earth surface processes in areas outside the polar regions, such as the Tibetan Plateau, could be investigated by the terrestrial ^{53}Mn method. A 5 g granodiorite sample (Fe $\approx$ 3.3 wt.%; Mn $\approx$ 0.07 wt.%) exposed for 100 ky at 4000 m in Tibet (30° N) is expected to yield 3.5 mg of manganese and a ratio of ^{53}Mn/^{55}Mn $= 1.0 \cdot 10^{-13}$.

We expect to further refine the terrestrial ^{53}Mn method. More production rate calibration experiments, further modelling, and experiments to refine the geochemistry as well as the AMS methods underlying this new tool are in progress. Finally, as samples brought back from Mars and other extraterrestrial bodies become available, ^{53}Mn may be, together with the cosmogenic noble gases, a valuable tool for addressing questions about geological processes on the Martian surface.

Acknowledgments

We appreciate the constructive reviews by Derek Vance and an anonymous reviewer. J.M.S. was supported by the NSF grant EAR-0345835 (CRONUS-Earth) and thanks the Comer Science and Educational Foundation for its support of this study. We are grateful to Roseanne Schwartz for her most competent help with the sample processing and Linda Baker for her assistance during the helium analysis. Work at Comenius University was supported by SGA grant and 6 F.P.grant CRONUS-EU. This is L-DEO contribution number 6959.

References

[1] J.C. Gosse, F.M. Phillips, Terrestrial in situ cosmogenic nuclides: theory and application, Quat. Sci. Rev. 20 (2001) 1475–1560.
[2] S. Niedermann, Cosmic-ray-produced noble gases in terrestrial rocks: dating tools for surface processes, in: D. Porcelli, C.J. Ballentine, R. Wieler (Eds.), Noble Gases in Geochemistry and Cosmochemistry, vol. 47, Mineralogical Society of America, 2002, pp. 731–784.
[3] T.E. Cerling, H. Craig, Geomorphology and in-situ cosmogenic isotopes, Annu. Rev. Earth Planet. Sci. Lett. 22 (1994) 273–317.
[4] N.A. Lifton, A.J.T. Jull, J. Quade, A new extraction technique and production rate estimate for in situ cosmogenic ^{14}C in quartz, Geochim. Cosmochim. Acta 65 (2001) 1953–1969.
[5] P.R. Renne, K.A. Farley, T.A. Becker, W.D. Sharp, Terrestrial cosmogenic argon, Earth Planet. Sci. Lett. 188 (2001) 435–440.
[6] M. Honda, J.R. Arnold, Effects of cosmic rays on meteorites, Handb. Phys. 46 (1967) 613–632.
[7] J.P. Shedlovsky, P.J.J. Cressy, T.P. Kohman, Cosmogenic radioactivities in the Peace River and Harleton chondrites, J. Geophys. Res. 72 (1967) 5051–5058.
[8] H.J. Millard, Thermal neutron activation: measurement of cross section for manganese-53, Science 147 (1965) 503–504.
[9] P.A.J. Englert, R. Sarafin, J. Masarik, R.C. Reedy, Cosmogenic ^{53}Mn in the main fragment of the Norton County aubrite, Geochim. Cosmochim. Acta 59 (1995) 825–830.
[10] U. Herpers, R. Sarafin, Determination of the spallogenic radionuclides Al-26 and Mn-53 in Antarctic meteorites with respect to cosmic ray exposure and terrestrial age, J. Radioanal. Nucl. Chem. 110 (1987) 191–195.
[11] M. Honda, K. Nishiizumi, M. Imamura, N. Takaoka, O. Nitoh, K. Horie, K. Komura, Cosmogenic nuclides in the Kirn chondrite, Earth Planet. Sci. Lett. 57 (1982) 101–109.
[12] K. Nishiizumi, M.T. Murrell, J.R. Arnold, Mn-53 profiles in four Apollo surface cores, Lunar and Planetary Science Conference XIV, J. Geophys. Res. (1983) B211–B219 (part 1).
[13] P. Englert, U. Herpers, R. Sarafin, S. Vogt, Exposure history of meteorites as deduced by sub-nanogram of manganese-53 radiochemical neutron activation analysis, J. Radioanal. Nucl. Chem. 113 (1987) 119–123.

[14] K. Knie, T. Faestermann, G. Korschinek, AMS at the Munich gas-filled analyzing magnet system GAMS, Nucl. Instrum. Methods Phys. Res., B Beam Interact. Mater. Atoms 123 (1997) 128–131.
[15] J.M. Schäfer, S. Ivy-Ochs, R. Wieler, I. Leya, H. Baur, G.H. Denton, C. Schlüchter, Cosmogenic noble gas studies in the oldest landscape on earth: surface exposure ages of the Dry Valleys, Antarctica, Earth Planet. Sci. Lett. 167 (1999) 215–226.
[16] M.D. Kurz, E.J. Brook, Surface exposure dating with cosmogenic nuclides, in: C. Beck (Ed.), Dating in Exposed and Surface Contexts, University of New Mexico Press, 1994, pp. 139–159.
[17] J.M. Schaefer, G. Herzog, S. Ivy-Ochs, K. Knie, G. Korschinek, P.W. Kubik, D.R. Marchant, C. Schluechter, F. Serefiddin, R. Wieler, News from the oldest ice on Earth buried in Antarctica, and a new cosmogenic tool, Geochim. Cosmochim. Acta 69 (2005) (Suppl. S.).
[18] F. Serefiddin, T. Faestermann, G.F. Herzog, K. Knie, G. Korschinek, J. Masarik, M. Poutivtsev, J.M. Schaefer, In-situ production rates of ^{53}Mn in Antarctic rocks, EOS Trans. AGU 85 (2004) (Fall Meet. Suppl., Abstract V51C-0596).
[19] G.H. Denton, D.E. Sugden, D.R. Marchant, B.L. Hall, T.I. Wilch, East Antarctic ice sheet sensitivity to Pliocene climatic change from a Dry Valleys perspective, Geogr. Ann. 75A (1993) 155–204.
[20] D.E. Sugden, G.H. Denton, D.R. Marchant, Landscape evolution of the Dry Valleys, Transantarctic Mountains: tectonic implications, J. Geophys. Res. 100 (1995) 9949–9967.
[21] F. Marcantonio, N. Kumar, M. Stute, R.F. Anderson, M.A. Seidl, P. Schlosser, A. Mix, A comparative study of accumulation rates derived by He and Th isotope analysis of marine sediments, Earth Planet. Sci. Lett. 133 (1995) 549–555.
[22] G. Winckler, R.F. Anderson, P. Schlosser, Equatorial Pacific productivity and dust flux during the Mid-Pleistocene climate transition, Paleoceanography 20 (2005) PA4025 (4010.1029/2005PA001177).
[23] C. Schnabel, P. Ma, G.F. Herzog, T. Faestermann, K. Knie, G. Korschinek, Be-10, Al-26, and Mn-53 in martian meteorites, Lunar and Planetary Science Conference, vol. XXXIV, 2001, Abstract #1353.
[24] S. Vogt, U. Herpers, Radiochemical separation techniques for the determination of long-lived radionuclide in meterorited by means of accelerator mass spectrometry, Fresenius Z. Anal. Chem. 331 (1988) 186–188.
[25] K. Knie, T. Faestermann, G. Korschinek, G. Rugel, W. Ruhm, A. Wallner, High-sensitivity AMS for heavy nuclides at the Munich Tandem accelerator, Nucl. Instrum. Methods, Sect. B (2000) 717–720.
[26] B. Brun, GEANT3 User's Guide, Rep. DD/EE/84-1, European Organisation for Nuclear Research, Geneva, 1987, p. 584.
[27] J.F. Briesmeister, MCNP-A General Monte Carlo N-particle Transport Code Version 4A, LA-12625-M, Los Alamos National Laboratory, Los Alamos, NM, 1993, p. 693.
[28] J. Masarik, J. Beer, Simulation of particle fluxes and cosmogenic nuclide production in the earth's atmosphere, J. Geophys. Res. D104 (1999) 12,099–13,012.
[29] J. Masarik, R.C. Reedy, Terrestrial cosmogenic-nuclide production systematics calculated from numerical simulations, Earth Planet. Sci. Lett. 136 (1995) 381–395.
[30] J. Stone, Air pressure and cosmogenic isotope production, J. Geophys. Res. 105 (2000) 23753–23759.
[31] L.A. Bruno, H. Baur, T. Graf, C. Schlüchter, P. Signer, R. Wieler, Dating of Sirius Group tillites in the Antarctic Dry Valleys with cosmogenic ^{3}He and ^{21}Ne, Earth Planet. Sci. Lett. 147 (1997) 37–54.
[32] J.M. Schäfer, Reconstruction of landscape evolution and continental paleoglaciations using in situ cosmogenic nuclides — examples from Antarctica and the Tibetan Plateau, Ph.D.-Thesis No. 13542, ETH Zürich, Switzerland, 2000.
[33] H.R. Margerison, W.M. Phillips, F.M. Stuart, D.E. Sugden, Cosmogenic ^{3}He concentrations in ancient flood deposits from the Coombs Hills, northern Dry Valleys, East Antarctica: interpreting exposure ages and erosion rates, Earth Planet. Sci. Lett. 230 (2005) 163–175.
[34] P. Oberholzer, Reconstructing paleoclimate and landscape history in Antarctica and Tibet with cosmogenic nuclides, Ph. D.-Thesis No 15472, ETH Zürich, 2004.
[35] S. Niedermann, J.M. Schaefer, R. Wieler, R. Naumann, Experimental determination of the cosmogenic Ar production rate from Ca, EOS Trans. AGU 86 (2005) (Fall Meet. Suppl., Abstract U33A-0003).
[36] B. Heisinger, E. Nolte, Cosmogenic in situ production of radionuclides: exposure ages and erosion rates, Nucl. Instrum. Methods Phys. Res., B Beam Interact. Mater. Atoms 172 (2000) 790–795.
[37] K. Nishiizumi, M.T. Murrell, J.R. Arnold, D. Elmore, R.D. Ferraro, H.E. Gove, R.C. Finkel, Cosmic-ray-produced Cl-36 and Mn-53 in Allan Hills-77 meteorites, Earth Planet. Sci. Lett. 52 (1981) 31–38.
[38] V.M. Goldschmidt, Geochemistry, Oxford University Press, Oxford, 1958 632–634 pp.
[39] S.-R. Jeon, J.H. Lee, Geochemistry of major and minor elements in a soil profile formed by weathering of granite; an example from the two-micra granite in the Jinan area, Jeonbuk, J. Geol. Soc. Korea 38 (2002) 293–307.
[40] F.M. Phillips, M.G. Zreda, D. Elmore, P. Sharma, A reevaluation of cosmogenic ^{36}Cl production rates in terrestrial rocks, Geophys. Res. Lett. 23 (1996) 949–952.
[41] J.O. Stone, G.L. Allan, L.K. Fifield, R.G. Cresswell, Cosmogenic chlorine-36 from calcium spallation, Geochim. Cosmochim. Acta 60 (1996) 679–692.
[42] T.W. Swanson, M.W. Caffee, Determination of ^{36}Cl production rates derived from the well-dated deglaciation surfaces of Whidbey and Fidalgo Islands, Washington, Quat. Res. 56 (2001) 366–382.
[43] P. Ma, G.F. Herzog, T. Faestermann, K. Knie, G. Korschinek, G. Rugel, A. Wallner, L. Schultz, J. Johnson, A.J.T. Jull, D. Fink, Exposure histories of seven ordinary chondrites with helium-3 losses, Lunar and Planetary Science Conference, vol. XXXIV, 2003, Abstract #1673.
[44] P.N. Webb, D.M. Harwood, B.C. McKelvey, J.H. Mercer, L.D. Stott, Cenozoic marine sedimentation and ice-volume variation on the East Antarctic craton, Geology 12 (1984) 287–291.
[45] F. Kober, S. Ivy-Ochs, I. Leya, H. Baur, T. Magna, R. Wieler, P.W. Kubik, In situ cosmogenic ^{10}Be and ^{21}Ne in sanidine and in situ cosmogenic ^{3}He in Fe–Ti-oxide minerals, Earth Planet. Sci. Lett. 236 (2005) 404–418.
[46] G.J. Feldman, R.D. Cousins, Unified approach to the classical statistical analysis of small signals, Phys. Rev., D 57 (1998) 3873–3889.